

Atomic Emission Spectra Using a UV-Vis Spectrophotometer and an Optical Fiber Guided Light Source

Manuel E. Minas da Piedade

Centro de Química Estrutural, Complexo I, Instituto Superior Técnico, 1096 Lisboa Codex, Portugal

Mário N. Berberan-Santos

Centro de Química-Física Molecular, Complexo I, Instituto Superior Técnico, 1096 Lisboa Codex, Portugal

The study of atomic emission spectra in the undergraduate laboratory has been suggested for many years to illustrate quantum mechanical principles (e.g., the idea that microscopic matter exists in quantized states) and the relation between the electronic structure and spectral observations (1–11). Because of the simplicity of its spectrum, hydrogen is by far the element of choice in published experiments in atomic spectroscopy (1–5, 8, 10, 11), but experiments involving other elements such as alkali metals have also been reported (6, 7, 9). Several types of apparatus have been used to record the spectra, including an atomic absorption spectrophotometer (1), spectroscopes (2–4), spectrographs (5–8) and UV-vis spectrophotometers (9–11). In all apparatuses of the latter type, the light source is either part of the spectrophotometer (deuterium lamp), yielding only a few lines (11), or when not a part, is placed inside the instrument (9, 10) and is therefore difficult to interchange. This makes impractical the study of more than one element in a laboratory session. As shown in the present paper, the use of an optical fiber to guide the light from an external source onto the monochromator of the spectrophotometer enables a fast sequential use of several light sources, irrespective of their size and shape. This setup has been in use in our undergraduate physical chemistry laboratory to study the emission spectra of hydrogen, sodium, and helium in a four-hour session. The experiment can be readily extended to other elements (e.g., Hg, Li, K, Xe, Ne) or modified to obtain molecular spectra from discharge tubes and lamps (e.g., N₂, D₂, H₂) and atomic and molecular spectra in flames (e.g., alkali metals, C₂), provided the appropriate light sources are available.

Apparatus

The apparatus used consists of a Perkin-Elmer Lambda 15 spectrophotometer, a plastic optical fiber with a diameter of 3.0 mm from Laser Components GmbH (PG-R-FB3000 Plastikfaser), and a light source. In the case of hydrogen and helium a light source from Electro-Technic Products, Inc., including a Spectrum tube power supply SP-200 (5 kV, 10 mA) and an interchangeable gas discharge lamp was used. The spectrum of sodium was recorded using a Bellingham+Stanley Ltd. sodium lamp unit removed from a polarimeter. The optical fiber is introduced into the spectrophotometer through a preexisting hole on the housing bottom and fixed by a clamp support near the entrance of the monochromator. Another clamp support is used to adjust the position of the fiber near the external light source. The hydrogen and helium light sources are placed at a distance of ca. 0.5 cm from the tip of the optical fiber in order to avoid damage to the fiber by the heat generated at the source lamp. In the case of the

much more intense sodium lamp, a longer distance (ca. 8 cm) is required to prevent photomultiplier saturation.

Recording the Spectra

The Perkin-Elmer Lambda 15 spectrophotometer is operated in the single-beam mode according to the manufacturer's instructions. A preliminary scan is made at a scan speed of 120 or 240 nm min⁻¹, to adjust the bandpass and gain so that the intensity of the stronger lines observed in the spectrum does not exceed ca. 100. To conveniently detect the weaker lines it may be necessary to record other spectra with increased bandpass and/or gain. In the case of sodium, for example, after the preliminary scan and the selection of convenient bandpass and gain, a global spectrum, without resolved doublets, is recorded. Then, slow scans at 7.5 nm min⁻¹ and bandpass = 0.25 nm are made in the near range of each unresolved line detected in the previous spectrum. It is then possible to observe fairly resolved doublets (well resolved only for the longer wavelengths, ca. $\lambda \geq 568$ nm).

The typical wavelength ranges covered in the experiment are 350–700 nm for hydrogen, 450–850 nm for sodium, and 350–750 nm for helium.

The wavelength calibration of the apparatus was checked with a mercury lamp from Electro-Technic Products, Inc.

Results and Discussion

Using the apparatus and experimental procedure described above, 8 lines (part of the Balmer series) are observed for hydrogen, at least 8 doublet lines are observed in the case of sodium, and a minimum of 15 lines are observed for helium. Because of the intrinsic absorption of the optical fiber used, the lowest measurable wavelength is about 350 nm. No special precautions are taken to eliminate the contamination by ambient light. Spectra obtained at high gains and with wide bandpasses may, however, show extraneous contributions (e.g., the strong mercury lines of fluorescent lamps in the laboratory ceiling).

Typical results obtained by the students for hydrogen are 379.8 nm (H_θ), 383.3 nm (H_η), 388.6 nm (H_ζ), 396.8 nm (H_ε), 410.0 nm (H_δ, h line), 433.6 nm (H_γ, G' line), 486.1 nm (H_β, F line), 656.3 nm (H_α, C line) (see ref 12 for assignments). Those for sodium and helium are shown in Tables 1 and 2 and in Figures 1 and 2. The intensities indicated in Tables 1 and 2 are not absolute, since the efficiencies of the optical system and of the photomultiplier of the spectrophotometer are wavelength dependent.

The students are asked to complete tasks described in the following sections.

Task 1

Assignment of the lines in the obtained spectra by comparison with literature data and construction of the Grotrian diagram (12–14) showing the energy levels and the observed transitions for hydrogen, sodium and helium (Figs. 3 and 4). Verification of the selection rules $\Delta l = \pm 1$ and $\Delta j = 0, \pm 1$ for hydrogen and sodium, and $\Delta l = \pm 1$ and $\Delta L = 0, \pm 1$, $\Delta S = 0$, $\Delta J = 0, \pm 1$ for helium, where l and L are the orbital angular momentum quantum numbers, j and J are the total angular momentum quantum numbers for atoms that can be considered as mono- (e.g., H and Na) and poly- (e.g., He) electron species, respectively, and S is the total spin angular momentum quantum number (12–14).

Task 2

Calculation of the Rydberg constant, \mathfrak{R}_H , and the ionization energy, IE, of hydrogen using the following equations (12–14):

$$\frac{1}{\lambda} = \mathfrak{R}_H \left(\frac{1}{n_1^2} - \frac{1}{n_2^2} \right) \quad (1)$$

$$\text{IE} = \mathfrak{R}_H hc \quad (2)$$

where λ represents the wavelength, $n_2 = 2$ (Balmer series), n_1 is an integer larger than n_2 , h is the Planck constant, and c is the velocity of light. A least squares fit of eq 1 to a plot of $1/\lambda$ vs $1/n_1^2$, using $n_1 = 3-10$ for $\lambda = 656.3-379.8$ nm, leads to $\mathfrak{R}_H = (1.0984 \pm 0.0024) \times 10^5 \text{ cm}^{-1}$. (All uncertainties quoted throughout this paper correspond to the standard deviation multiplied by Student's t parameter for a 95% confidence level.) This result is in good agreement with the theoretical value $\mathfrak{R}_H = 109,677.6 \text{ cm}^{-1}$ (calculated from 12–14):

$$\mathfrak{R} = \frac{\mu e^4}{8\epsilon_0^2 h^3 c} \quad (3)$$

where e represents the elementary charge, ϵ_0 is the vacuum permittivity, h is the Planck constant, c is the velocity of light, and μ is the reduced mass of the nucleus + electron system given by

$$\mu = \frac{m_N m_e}{m_N + m_e} \quad (4)$$

where m_N and m_e are the masses of the nucleus and of the electron, respectively. From the obtained Rydberg constant, $(1.0984 \pm 0.0024) \times 10^5 \text{ cm}^{-1}$, and eq 2 it is possible to conclude that for hydrogen $\text{IE} = 13.62 \pm 0.03 \text{ eV}$, in good agreement with the value $\text{IE} = 13.59844 \text{ eV}$ recommended in ref 15. It should be noted that for more accurate work the conversion of the experimental wavelengths, measured in air, to the corresponding values in vacuum must be taken into account (8, 12). In our case, however, this correction is well within the experimental error and was therefore neglected.

Task 3

Calculation of the Rydberg constant and of the ionization energy of sodium. Calculation of the quantum defect corrections for the sharp (S, $n_s \rightarrow 3p$), principal (P, $n_p \rightarrow 3s$),

Table 1. Wavelengths and Intensities of Atomic Sodium Emission Lines

Observed	λ/nm (in air)		Intensity/ arbitrary units
	Assignment (12)	Deviation	
466.6 ^a	466.5 ($6^2D_{5/2,3/2} \rightarrow 3^2P_{1/2}$)	-0.1 ^b	19
	466.9 ($6^2D_{5/2,3/2} \rightarrow 3^2P_{3/2}$)		
474.9 ^a	474.8 ($7^2S_{1/2} \rightarrow 3^2P_{1/2}$)	-0.1 ^b	4
	475.2 ($7^2S_{1/2} \rightarrow 3^2P_{3/2}$)		
498.0 ^a	497.9 ($5^2D_{5/2,3/2} \rightarrow 3^2P_{1/2}$)	-0.1 ^b	104
	498.3 ($5^2D_{5/2,3/2} \rightarrow 3^2P_{3/2}$)		
515.1 ^a	514.9 ($6^2S_{1/2} \rightarrow 3^2P_{1/2}$)	-0.1 ^b	23
	515.4 ($6^2S_{1/2} \rightarrow 3^2P_{3/2}$)		
568.1	568.3 ($4^2D_{5/2,3/2} \rightarrow 3^2P_{1/2}$)	-0.2	130
568.6	568.8 ($4^2D_{5/2,3/2} \rightarrow 3^2P_{3/2}$)	-0.2	
588.8	589.0 ($3^2P_{3/2} \rightarrow 3^2S_{1/2}$)	-0.2	139
	D ₂ line		
589.4	589.6 ($3^2P_{1/2} \rightarrow 3^2S_{1/2}$)	-0.2	
	D ₁ line		
615.3	615.4 ($5^2S_{1/2} \rightarrow 3^2P_{1/2}$)	-0.1	67
616.0	616.1 ($5^2S_{1/2} \rightarrow 3^2P_{3/2}$)	-0.1	
818.1	818.3 ($3^2D_{5/2,3/2} \rightarrow 3^2P_{1/2}$)	-0.2	90
819.2	819.5 ($3^2D_{5/2,3/2} \rightarrow 3^2P_{3/2}$)	-0.3	129

^aUnresolved doublet. ^bCalculated using the average doublet wavelength.

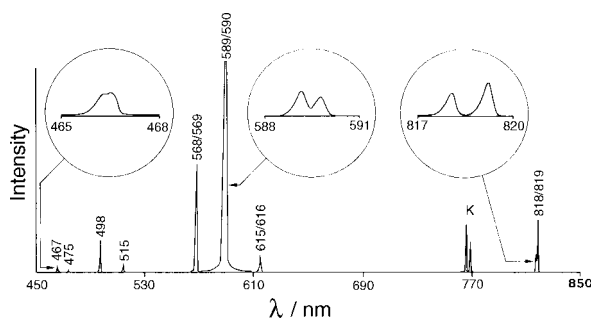


Figure 1. Sodium emission spectrum (see Table 1 for assignments and relative intensities). The observed doublet structure recorded at 7.5 nm min^{-1} is shown for selected lines. K is the resonance doublet from a potassium impurity.

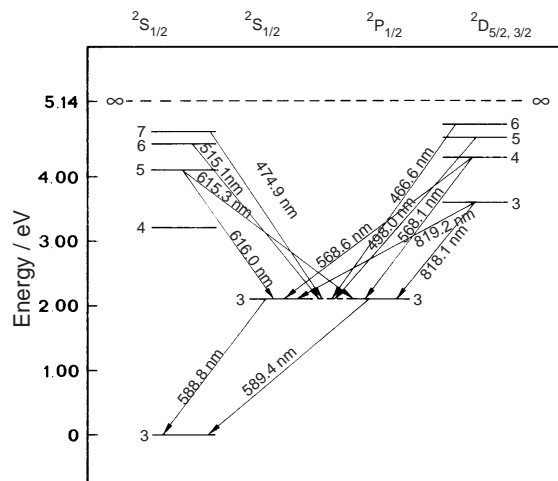


Figure 3. Grotrian diagram for sodium showing the transitions observed in the laboratory (see also Table 1). The transitions at 466.6, 474.9, 498.0, and 515.1 nm correspond to unresolved doublets.

Table 2. Wavelengths and Intensities of Helium Emission Lines

λ/nm (in air)		Intensity/ arbitrary units
Observed	Assignment (12)	
361.0	361.3 (5 $^1P_1 \rightarrow 2^1S_0$)	4 ^a
388.7	388.9 (3 $^3P_{2,1,0} \rightarrow 2^3S_1$)	64 ^b
396.2	396.5 (4 $^1P_1 \rightarrow 2^1S_0$)	26 ^a
402.4	402.6 (5 $^3D_{3,2,1} \rightarrow 2^3P_{2,1,0}$)	2 ^b
411.9	412.1 (5 $^3S_1 \rightarrow 2^3P_{2,1,0}$)	8 ^a
438.6	438.8 (5 $^1D_2 \rightarrow 2^1P_1$)	12 ^a
446.9	447.2 (4 $^3D_{3,2,1} \rightarrow 2^3P_{2,1,0}$)	19 ^b
471.1	471.3 (4 $^3S_1 \rightarrow 2^3P_{2,1,0}$)	4 ^b
492.0	492.2 (4 $^1D_2 \rightarrow 2^1P_1$)	5 ^b
501.4	501.6 (3 $^1P_1 \rightarrow 2^1S_0$)	25 ^b
504.5	504.8 (4 $^1S_0 \rightarrow 2^1P_1$)	15 ^a
587.5	587.6 (3 $^3D_{3,2,1} \rightarrow 2^3P_{2,1,0}$) D ₃ line	72 ^b
667.7	667.8 (3 $^1D_2 \rightarrow 2^1P_1$)	23 ^b
706.4	706.6 (3 $^3S_1 \rightarrow 2^3P_{2,1,0}$)	32 ^b
728.0	728.1 (3 $^1S_0 \rightarrow 2^1P_1$)	18 ^a

^aBandpass = 2 nm, gain = 25. ^bBandpass = 1 nm, gain = 25.

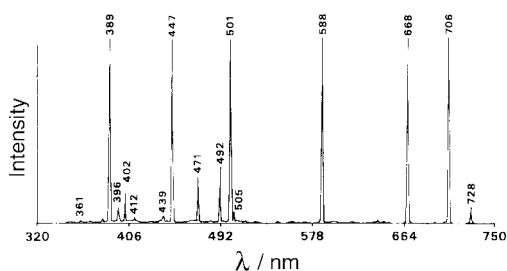


Figure 2. Helium emission spectrum (see Table 2 for assignments and relative intensities).

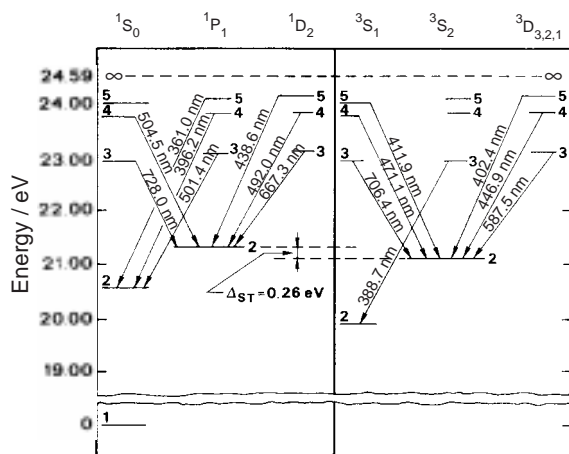


Figure 4. Grotrian diagram for singlet (a) and triplet (b) helium showing the transitions observed in the laboratory. The corresponding wavelengths are given in Table 2.

and diffuse (D, $nd \rightarrow 3p$) series of sodium. Analysis of the doublet structure of the sodium lines.

The analogue of eq 1 for sodium is the empirical equation (12–14)

$$\frac{1}{\lambda} = -\mathfrak{R}_{\text{Na}} \left[\frac{1}{(n_1 - \delta_{n_1 l_1})^2} - \frac{1}{(n_2 - \delta_{n_2 l_2})^2} \right] \quad (5)$$

where \mathfrak{R}_{Na} is the Rydberg constant for sodium, $n_2 = 3, 4,$ and 5 for the P, D, and S series, respectively, n_1 is an integer equal to or larger than n_2 , and $\delta_{n_1 l_1}$ and $\delta_{n_2 l_2}$ are the quantum defects or Rydberg corrections. The quantum defect is related to the interaction of the electron whose transitions produce the spectrum with the inner core electrons; it is approximately constant for levels of different principal quantum number, n , but with the same orbital angular momentum quantum number, l (i.e., for the same series) (12–14). The value of the quantum defect increases with the degree of penetration of the corresponding orbital. It takes, therefore, the highest values for the S series and is close to zero for the D series (see below).

Equation 5 was separately fitted to the data of the diffuse and sharp series shown in Table 1, in the form

$$\frac{1}{\lambda} = \frac{A}{(n_1 - B)^2} + C \quad (6)$$

where A , B , and C are the fitting parameters, given by

$$A = -\mathfrak{R}_{\text{Na}} \quad (7)$$

$$B = \delta_{n_1 l_1} \quad (8)$$

$$C = \frac{\mathfrak{R}_{\text{Na}}}{(n_2 - \delta_{n_2 l_2})^2} \quad (9)$$

The values of these parameters were found by using the Solver tool of MS Excel 7.0 to minimize the sum of the squares of the deviations between calculated and experimental wavelengths (Table 3). The uncertainties of the parameters are not determined in the case of this nonlinear fit. This can be done by Monte Carlo simulation (16), but the calculation is beyond the scope of this laboratory experiment. Comparison of the results obtained for H, Na, and He, with the corresponding (more accurate) literature values, however, allows a posteriori estimation of the accuracy of the Rydberg constants and quantum defects obtained from eq 6. Accuracies better than 1% are found for the Rydberg constants, and in the case of the quantum defects two to three exact decimal places are observed. From the data in Table 3 and eqs 6–9 it is possible to conclude that for the diffuse series $\delta_{n,d} = 0.000$, $\delta_{3p} = 0.876$, and $\mathfrak{R}_{\text{Na}} = 110,514 \text{ cm}^{-1}$. These results are in good agreement with those reported by Stafford and Wortman, which assumed that $\delta_{n,d} = 0$ and used a linear adjustment of eq 5 to a $1/\lambda$ vs. $1/n^2$ plot to derive $\delta_{3p} = 0.88$ and $\mathfrak{R}_{\text{Na}} = 110,600 \text{ cm}^{-1}$ (9). Note, however, that the Rydberg constant obtained in the present experiment, $\mathfrak{R}_{\text{Na}} = 110,514 \text{ cm}^{-1}$, is too high when compared to its theoretical value $\mathfrak{R}_{\text{Na}} = 109,734.7 \text{ cm}^{-1}$ cal-

culated from eq 3. In addition, the quantum defect for the 3p level, $\delta_{3p} = 0.876$, is lower than the value $\delta_{3p} = 0.883$ recommended in (12, 14, 17). For these reasons, a constrained adjustment of eq 5 to the experimental data, with $\mathfrak{R}_{\text{Na}} = 109,734.7 \text{ cm}^{-1}$, was also carried out. A slightly worse fit (maximum deviation equal to 0.1 nm) was obtained, yielding quantum defects $\delta_{nd} = 0.009$ and $\delta_{3p} = 0.883$, in very good agreement with the published values $\delta_{nd} = 0.01$ and $\delta_{3p} = 0.883$ (12, 14, 17). For the sharp series, the best fit (Table 3) gave quantum defects $\delta_{ns} = 1.36$ and $\delta_{3p} = 0.885$, and a Rydberg constant $\mathfrak{R}_{\text{Na}} = 109546 \text{ cm}^{-1}$; but imposing again $\mathfrak{R}_{\text{Na}} = 109734.7 \text{ cm}^{-1}$ yields quantum defects, $\delta_{ns} = 1.36$ and $\delta_{3p} = 0.883$, in better agreement with the literature values $\delta_{ns} = 1.36$ and $\delta_{3p} = 0.883$ (12, 14, 17). Note, finally, that since not all the doublets of each sodium line were well resolved in the obtained spectrum, the mean wavelength value of each doublet in Table 1 was selected for the calculations. For a more accurate calculation the wavelengths of just one of the two spin-orbit components should be used.

The magnitude of the spin-orbit coupling can also be evaluated for the resolved doublet lines. In the case of the D line, for example, a spin-orbit coupling of 17.3 cm^{-1} is obtained from the experimental data in Table 1. This result is in good agreement with the published value of 17.2 cm^{-1} (12). It is also interesting to note that a very well resolved doublet line from a potassium impurity is observed in the spectrum of sodium at wavelengths 766.3 and 769.7 nm. This doublet is the equivalent in potassium of the sodium D line. In this case, a spin-orbit coupling of 57.6 cm^{-1} is calculated, in good agreement with the published value of 57.7 cm^{-1} (12). The strong dependence of the spin-orbit coupling on the atomic number Z —it increases with Z^4 (12–14)—is clearly seen by comparing the obtained results for sodium and potassium indicated above (17.3 cm^{-1} and 57.6 cm^{-1} , respectively).

Another possible topic of discussion is the relative intensity of the two components of the doublet lines. For instance, in the case of the D line, the theoretical ratio between the intensities of the $P_{3/2} \rightarrow S_{1/2}$ and $P_{1/2} \rightarrow S_{1/2}$ components is 2:1; that is, that of the statistical weights ($2j + 1$) of the corresponding upper states (12). For most commercial lamps the measured ratio is frequently lower owing to the reabsorption phenomenon (12), which is important when the concentration of the sodium atoms is high. In our case a ratio of 1.3:1 is observed (Fig. 1). If, however, the D line doublet spectrum is recorded immediately after turning the lamp on (when the concentration of Na in the vapor is low) the theoretical ratio of 2:1 is indeed observed.

The first ionization energy of ground-state sodium can also be calculated from the spectral data (12–14). In this calculation it is assumed that the ionization process can be decomposed in two steps: in the first one, ground-state sodium is excited to the 3^2P state (energy required = $h\nu = 2.11 \text{ eV}$, where ν is the frequency of the D line); in the second, sodium in the 3^2P state is further excited to the ionization limit. The energy required for this second step corresponds to the limit $n_2 \rightarrow \infty$ of eq 5 and is thus given by the constant C of eq 6. Conversion of the C values in Table 3 to eV leads to $C = 3.04 \text{ eV}$. Thus, $IE_{\text{Na}} = 5.15 \text{ eV}$ is derived, in good agreement with the recommended value, $IE_{\text{Na}} = 5.13908 \text{ eV}$ (15).

Table 3. Best-Fit Values of A, B, and C Parameters (Eq 6) for Sodium D and S Series

Series	$-A/\text{cm}^{-1}$	B	C/cm^{-1}
D	110,514	0.000	24,505
S	109,546	1.359	24,489

Task 4

Calculation of the Rydberg constant and the ionization energy of helium. Calculation of the singlet–triplet gap for the 2P states.

In the case of helium singlet and triplet D series the following empirical equation is valid (12):

$$\frac{1}{\lambda} = -\mathfrak{R}_{\text{He}} \left[\frac{1}{n_1^2} - \frac{1}{(n_2 - \delta_{3p})^2} \right] \quad (10)$$

where \mathfrak{R}_{He} is the Rydberg constant for helium, $n_1 = 3, 4$, and 5, $n_2 = 2$, and δ_{3p} represents the quantum defect for the singlet or triplet 3P state. According to eq 10, a plot of $1/\lambda$ versus $1/n_1^2$ should give a straight line of slope $-\mathfrak{R}_{\text{He}}$ and intercept $\mathfrak{R}_{\text{He}}/(2 - \delta_{3p})^2$. Least square fits to the results in Table 2 lead to $\mathfrak{R}_{\text{He}} = 110,000 \pm 100 \text{ cm}^{-1}$ and $\delta_{3p} = -0.011$ for the singlet series and $\mathfrak{R}_{\text{He}} = 110,100 \pm 600 \text{ cm}^{-1}$ and $\delta_{3p} = 0.060$ for the triplet series. The corresponding values in ref 12 are $\mathfrak{R}_{\text{He}} = 109,722 \text{ cm}^{-1}$ and $\delta_{3p} = -0.009$ and 0.063 for the singlet and triplet series, respectively.

The ionization energies of the 2^1P and 2^3P states can also be calculated from the intercepts of the least square fits referred to above. The obtained values, $3.37 \pm 0.01 \text{ eV}$ for 2^1P and $3.63 \pm 0.01 \text{ eV}$ for 2^3P states, are in excellent agreement with the corresponding values in ref 12, 3.370 eV (2^1P) and 3.624 eV (2^3P), respectively, and lead to a singlet–triplet gap of 0.26 eV .

As for sodium, the ionization energy of ground-state helium can be calculated by adding the energy of the $2^1P_1 - ^1S_0$ transition (21.23 eV), which in this case is taken from the literature (12), to the ionization energy of the 2^1P state indicated above (3.37 eV). This leads to $IE_{\text{He}} = 24.60 \text{ eV}$, in good agreement with the value 24.58741 eV recommended in ref 15.

Concluding Remarks

The experiment described is fast (a four-hour session) and simple and yields accurate results. It illustrates a number of important topics in atomic structure and atomic spectroscopy that are covered in all undergraduate physical chemistry courses but often not studied in the laboratory owing to the lack of appropriate equipment. The required apparatus is assembled with common instruments (polarimeter or refractometer sodium lamp and a UV–vis spectrophotometer), the additional equipment required being only a plastic optical fiber, low-cost hydrogen and helium discharge tubes, and appropriate power supply. It can also be used to obtain molecular spectra from discharge tubes or lamps (e.g., N_2 , D_2 , H_2) and

atomic and molecular spectra in flames (e.g., alkali metals, C_2). Finally, the present laboratory experiment can motivate the discussion of more advanced topics in atomic spectroscopy, such as the hydrogen fine structure (14, 18) and Rydberg states (14, 19), and of the working principles of spectroscopic components, such as discharge tubes (20), optical fibers (21), monochromators (8, 22), and photomultiplier detectors (8).

Literature Cited

1. Douglas, J.; von Nagy-Felsobuki, E. I. *J. Chem. Educ.* **1987**, *64*, 552.
2. Companion, A.; Schug, K. *J. Chem. Educ.* **1966**, *43*, 591.
3. Reiss, E. *J. Chem. Educ.* **1988**, *65*, 517.
4. Shields, G. C.; Kash, M. M. *J. Chem. Educ.* **1992**, *69*, 329.
5. Rappon, M.; Greer, J. M. *J. Chem. Educ.* **1987**, *64*, 453.
6. McSwiney, H. D.; Peters, D. W.; Griffith, W. B., Jr.; Mathews, C. W. *J. Chem. Educ.* **1989**, *66*, 857.
7. Miller, K. J. *J. Chem. Educ.* **1974**, *51*, 805.
8. Shoemaker, D. P.; Garland, C. W.; Nibler, J. W. *Experiments in Physical Chemistry*, McGraw-Hill: New York, 1989.
9. Stafford, F. E.; Wortman, J. H. *J. Chem. Educ.* **1962**, *39*, 630.
10. Hollenberg, J. L. *J. Chem. Educ.* **1966**, *43*, 216.
11. Guiñón, J. L. *J. Chem. Educ.* **1989**, *66*, 790.
12. Kuhn, H. G. *Atomic Spectra*; Longmans: London, 1964.
13. Softley, T. P. *Atomic Spectra*, Oxford Chemistry Primers Series; Oxford University Press: New York, 1994.
14. Haken, H.; Wolf, H. C. *The Physics of Atoms and Quanta*, 5th ed.; Brewer, W. D., transl.; Springer: Berlin, 1996.
15. *Handbook of Chemistry and Physics*, 74th ed.; Lide, D. R., Ed.; CRC: Boca Raton, 1993–94.
16. Press, W. H.; Teukolsky, S. A.; Vetterling, W. T.; Flannery, B. P. *Numerical Recipes*, 2nd ed.; Cambridge University Press: Cambridge, 1992.
17. Slater, J. C. *Quantum Theory of Atomic Structure*, Vol. I; McGraw-Hill: New York, 1960.
18. Powell, R. E. *J. Chem. Educ.* **1968**, *45*, 558.
19. Silverman, M. P. *And Yet it Moves—Strange Systems and Subtle Questions in Physics*; Cambridge University Press: Cambridge, 1993.
20. Lewin, S. Z. *J. Chem. Educ.* **1965**, *42*, A165.
21. Melliar-Smith, C. M. *J. Chem. Educ.* **1980**, *57*, 574.
22. Guiñón, J. L.; Garcia-Anton, J. *J. Chem. Educ.* **1992**, *69*, 77.